JOURNAL OF Materials CHEMISTRY

A new approach to the synthesis of molybdenum bimetallic nitrides and oxynitrides

Silvia Alconchel,† Fernando Sapiña,* Daniel Beltrán and Aurelio Beltrán

Institut de Ciència dels Materials de la Universitat de València C/Doctor Moliner 50, 46100 Burjassot, Spain. E-mail: fernando.sapina@uv.es

Received 6th November 1998, Accepted 14th December 1998

A simple processing route to molybdenum bimetallic nitrides and oxynitrides has been developed, based on the use of precursors resulting from freeze-drying of aqueous solutions of the appropriate common metal salts. Thermal decomposition of amorphous freeze-dried powders originates crystalline mixed oxides, which have been carefully characterized. Nitridation of the crystalline intermediate having Ni : Mo = 2 : 3 metal ratio led to single-phased Ni_2Mo_3N. For the V–Mo–O–N system, nitridation of both amorphous and crystalline precursors results in bimetallic oxynitrides. In this way, not only the already known $V_2Mo(O_xN_y)$ catalyst but also a new compound of different metal stoichiometry, $V_3Mo_2(O_xN_y)$, has been prepared. The materials have been characterized by X-ray powder diffraction, elemental analysis, scanning electron microscopy, thermogravimetry under air flow, and temperature programmed oxidation. The existence of a solid solution of stoichiometry $V_{1-z}Mo_z(O_xN_y)$ $(0 \leqslant z \leqslant 1)$ having rock-salt structure is discussed.

Introduction

In a recent publication concerning the chemistry of interstitial molybdenum nitrides,[1] we referred to the renewed interest in transition-metal carbides and nitrides as more applications for these materials emerge.[2] Mono- and bi-metallic transition metal nitrides and oxynitrides are receiving considerable attention in the field of catalysis owing to the exceptional reactivity shown by some of them.[3] In this context, it is well known that the preparative route plays a critical role in the properties of the reaction products, controlling the structure, morphology, grain size and surface area of the obtained materials.[4] Thus, there are several synthetic approaches which have been used to obtain bimetallic nitrides and oxynitrides. Examples include the direct reaction of a metal nitride with a metal or another metal nitride, the reaction of a mechanical mixture of two metal powders with nitrogen or ammonia, the reaction between a metal amide with a metal or a metal nitride at low pressures (under flowing nitrogen or ammonia) or at high pressures (autoclave), and the ammonolysis of mixed metallic oxides.[5] Concerning catalytic properties, the use of bimetallic mixed oxide precursors (as an alternative to conventional solid state reactions) offers the advantage of atomic-level mixing of the metals, which decreases the diffusion distances of the cations and may lower the temperature necessary for reaction.[6] This procedure presents, however, an inherent limitation: the stoichiometric ratio of the metals in the resulting product (considered as a whole) being the same as that initially present in the precursor, the presence of impurities together with the main phase will usually occur when the metal proportion in the nitride differs from that of the starting oxide. In practice, this was our observation upon isolation of a molybdenum–nickel ternary nitride by ammonolysis of nickel molybdate.[1] Thus, regardless of the utility of this procedure when treating with some well established compositions, it is desirable to design alternative synthetic methods in order to explore different metal compositions in complex systems. One such alternative procedure that has been recently reported is based on the ammonolysis of metallorganic hydroxide precursors.[7] Whereas it has been successfully applied for the synthesis of several bimetallic nitrides, the treatments described are intricate being multi-step and prolonged. On the other hand, the use of polymetallic precursors resulting from freeze-drying of aqueous solutions has already proved to be a powerful technique to overcome the problem of stoichiometry in the case of complex oxides, such as high T_c superconducting materials,[8] although differences in the chemical activity of the components of the involved systems might affect procedural variables. It should be also considered that solution procedures appear especially suitable for the preparation of supported catalysts.

In the present work, we report how the use of freeze-dried polymetallic precursors has allowed us to overcome the above mentioned stoichiometric problem hindering the preparation of Ni_2Mo_3N as a single phase. In the same way, we have been able to prepare two different vanadium molybdenum oxynitrides, $V_2Mo(O_xN_y)$ and $V_3Mo_2(O_xN_y)$. In practice, $V_2Mo(O_xN_y)$ has specifically attracted considerable attention because of its exceptional catalytic activity in processes involving hydrogen transfer reactions.[9,10]

Experimental

Synthesis

Materials used as reagents in the current investigation were $NiC_4H_6O_4{\cdot}4H_2O$ (Fluka, >99%), NH_4VO_3 (BDH Chemicals, 98%), V_2O_5 (Aldrich, 99.6%), $(NH_4)_6Mo_7O_{24}{\cdot}4H_2O$ (Panreac, 99.0%) and MoO_3 (Merck, 99.5%). Starting Ni, V or Mo containing solutions were prepared by dissolving their respective salts in distilled water. Then, they were combined to obtain Ni–Mo and V–Mo source solutions whose total cationic concentrations were 0.25 and 0.50 M, respectively. The masses of the different reagents were adjusted to give 5 g of the final products. In the case of the Ni–Mo solution, to avoid precipitation, a small amount of acetic acid was added to the starting Mo solution (until pH *ca.* 3–4) before mixing. The compositions of these source solutions were prepared to have metal ratios Ni : Mo = 2 : 3, and V : Mo = 2 : 1 or 3 : 2. Droplets of these solutions were flash frozen by projection on liquid nitrogen and then freeze-dried at a pressure of 1–10 Pa in a Telstar Cryodos freeze-drier. In this way, dried solid precursors were obtained as amorphous (X-ray diffraction) loose powders. Crystalline mixed oxides were in turn obtained by heating

†Permanent address: Departamento de Química General e Inorgánica, Facultad de Ingeniería Química, Universidad Nacional del Litoral, Santiago del Estero 2829, 3000 Santa Fe, Argentina.

Table 1 Chemical composition of single-phase powder nitrides and oxynitrides

Sample	Precursor[a]	M(at.%)/ Mo(at.%)[b]	Oxygen (wt.%)	Nitrogen (wt.%)	Stoichiometry proposed
NiMoN-A	Crystalline	0.64 (0.67)	0.19	3.34	Ni_2Mo_3N
VMoN-A	Amorphous	1.92 (2.0)	9.0	13.6	$V_2Mo(O_{1.4}N_{2.5})$
VMoN-B	Crystalline	1.90 (2.0)	7.7	12.7	$V_2Mo(O_{1.2}N_{2.3})$
VMoN-C	Ceramic	1.97 (2.0)	10.0	13.5	$V_2Mo(O_{1.6}N_{2.5})$
VMoN-D	Amorphous	1.47(1.5)	7.0	13.3	$V_3Mo_2(O_{1.9}N_{4.1})$
VMoN-E	Crystalline	1.44 (1.5)	6.3	12.5	$V_3Mo_2(O_{1.7}N_{3.8})$

[a]Amorphous precursor: freeze-dried powder. Crystalline precursors: as resulting from the thermal decomposition of the amorphous precursors in air. Ceramic precursor: crystalline solid obtained by the ceramic method. [b]Expected values, according to nominal stoichiometry, in parentheses.

the amorphous precursors for 3 h under air at 873 K (Ni–Mo) or 723 K (V–Mo).

For comparison, a crystalline V–Mo mixed oxide was also prepared by solid state reaction of vanadium(v) oxide and molybdenum(vi) oxide in a V : Mo ratio of 2 : 1. Both monometallic oxides were first ground together using ball milling with added propan-2-ol to achieve better dispersion. The mixture was then dried and fired at 873 K for 8 h. Once the solid was cooled to room temperature, it was removed from the furnace, ground, and subjected again to the same thermal treatment.

Ni–Mo nitrides and V–Mo oxynitrides were synthesized by ammonolysis of the precursors, using in different preparations amorphous or crystalline precursor solids (Table 1). The gases employed were NH_3 (99.9%) and N_2 (99.9995%). A sample of the selected precursor (*ca.* 0.5 g) was placed into an alumina boat, which was then inserted into a quartz flow-through tube furnace. The back end of the tube furnace was connected to an acetic acid trap and the front end was connected to the gas line or to a vacuum pump. Prior to initiating the thermal treatment, the tube furnace was evacuated under vacuum for 20 min, then purged for 10 min with N_2 and another 20 min with NH_3. The precursor powder was heated at 5 K min^{-1} under flowing ammonia (50 cm^3 min^{-1}) to a final temperature of 1223 K for Ni–Mo samples or 1038 K for V–Mo samples. The samples were held at the reaction temperature for 4 h for Ni–Mo and 2 h for V–Mo, and then quenched to room temperature by turning off and opening the furnace. After cooling, the resulting solid was purged with N_2 for 10 min. All products were stored in a desiccator over $CaCl_2$.

Characterization

Elemental analysis. Metal ratios in the solids were determined by energy dispersive analysis of X-rays (EDAX) on a JEOL JSM 6300 scanning electron microscope, that were collected by an Oxford detector with quantification performed using virtual standards on associated Link-Isis software. The operating voltage was 20 kV, and the energy range of the analysis 0–20 keV. The nitrogen content of the nitrides and oxynitrides was evaluated by standard combustion analysis (Carlo Erba EA 1108). The oxygen content was determined by pyrolysis at 1343 K over nickelated carbon using a Carlo Erba 1500 elemental analyzer; N_2 and CO were separated in a chromatographic column, and measured using a thermal conductivity detector. The oxygen content was also indirectly tested by thermogravimetric analysis (Perkin Elmer TGA 7 system). Table 1 summarizes the results of these analyses for the resulting nitrides and oxynitrides.

X-Ray diffraction. X-Ray powder diffraction patterns were obtained from a Seifert C-3000 θ–θ automated diffractometer using graphite-monochromated Cu-Kα radiation. Powder samples were mixed with acetone to form a slurry and mounted on a glass slide. Routine patterns for phase identification were collected with a scanning step of 0.08° 2θ over the angular range 10–70° 2θ with a collection time of 3 s $step^{-1}$.

Table 2 Structural data from X-ray powder diffraction studies of Ni_2Mo_3N

Atom	Wyckoff	x	y	z
Ni(1)	8c	0.18318(15)	0.18318(15)	0.18318(15)
Mo	12d	0.79821(7)	0.04821(7)	1/8
N	4b	7/8	7/8	7/8

Space group, $P4_132$, $a = 6.63399(3)$ Å. $R_p = 10.1$, $R_{wp} = 12.8$, $R_B = 3.45$, $R_F = 2.58$.

For Rietveld analysis of Ni_2Mo_3N, the pattern was collected with a scanning step of 0.02° 2θ, over a wider angular range (20–140° 2θ), and with a longer acquisition time (10 s $step^{-1}$) in order to enhance statistics. Rietveld analysis was performed with the FULLPROF program.[11] The fits were performed using a pseudo-Voigt peak-shape function. In the final runs, usual profile parameters (scale factors, background coefficients, zero-points, half-width, pseudo-Voigt and asymmetry parameters for the peak-shape) and atomic positions were refined. Isotropic thermal parameters were set at 0.3 and 0.7 $Å^2$ for metals and nitrogen atoms, respectively, and an overall thermal parameter was also refined. Residuals given in Table 2 are the conventional (background corrected) peak only Rietveld profile and weighted profile residuals, R_p and R_{wp}, and the integrated intensity and structure factor residuals, R_B and R_F. A selected list of bond distances is summarized in Table 3. It must be stressed that, for a better estimation of the accuracy of the parameters, the standard deviations (that relate only to the precision of parameters), must be multiplied by the SCOR parameter,[12] which has a value of 2.24. All the graphical representations concerning X-ray powder diffraction patterns were performed using the DRXWin program.[13]

Microstructural characterization. The morphology of both the crystalline precursors and the resulting nitrides and oxynitrides was observed using a scanning electron microscope (Hitachi S-4100) operating at an accelerating voltage of 30 kV. The powders were dispersed in ethanol and treated with ultrasound for 10 min. All the preparation samples were covered with a thin film of gold for better image definition.

Oxidation behavior. In addition to thermogravimetric measurements, temperature-programmed oxidation of the nitrides and oxynitrides was carried out using a Micromeritics TPD/TPR 2900 instrument equipped with a thermal conductivity detector. In a typical TPO experiment, 50 mg of the powder were contacted with the reactant 2% (v/v) O_2–He flow

Table 3 Selected bond distances (in Å) for Ni_2Mo_3N

Ni–Ni ×3	2.4692(15)	Mo–Mo ×4	2.7767(6)
Ni–Mo ×3	2.7337(12)	Mo–Mo ×2	2.8146(6)
Ni–Mo ×3	2.7384(12)	N–Mo ×6	2.0810(3)
Ni–Mo ×3	2.8174(12)		

($50\ cm^3\ min^{-1}$), while the temperature was raised at $5\ K\ min^{-1}$.

Results and discussion

Ni–Mo–N system

As we have recently shown, the ternary nickel molybdenum nitride obtained by high temperature ammonolysis of nickel molybdate, $NiMoO_4$, has the stoichiometry Ni_2Mo_3N.[1] This way, the difference in stoichiometry between the precursor and the final nitride systematically resulted in the presence of impurities, which very likely are the basis of erroneous results previously reported in the literature which referred to a non-existent 'Ni_3Mo_3N' nitride.[6d,7a] At this point, the goal of obtaining single-phase Ni_2Mo_3N was the purpose of the synthetic approach presented in this work.[14] Obviously, the first preparative requirement was to think about alternative precursors containing the correct Ni : Mo ratio, which led us to assay the use of polymetallic precursors resulting from the freeze-drying of aqueous solutions. Thus, we carried out ammonolysis procedures, under conditions similar to those reported as optimal in ref. 1, using as precursors both the amorphous solid (as resulting from freeze-drying of the acetic solution) and the crystalline solid obtained by the thermal treatment of the amorphous freeze dried solid.

Thermal treatment of the amorphous precursor at 873 K during 3 h under air led to a yellowish green solid the X-ray diffraction pattern of which indicates that is a mixture of $NiMoO_4$ (JCPDS 33,0948) and MoO_3 (JCPDS 35,0609). Independent TGA experiments showed that such a transformation, which occurs with an associated weight loss close to 40%, is practically complete at *ca.* 600 K. MoO_3 is eliminated by sublimation above 950 K, and no formation of any new mixed oxide phase is detected over the entire process.

A metallic-grey solid was obtained as result of the ammonolysis of the amorphous precursor (1223 K, 4 h). Its X-ray diffraction pattern shows that it is a mixture in which the majority phases are Ni_2Mo_3N,[1] $Ni_{0.2}Mo_{0.8}N$ (JCPDS 29,0931) and Ni_3N (JCPDS 10,0280). The pattern includes also peaks previously attributed to an unidentified impurity having a cubic cell with an *a* parameter of 3.590 Å.[1]

The results of the ammonolysis of the crystalline precursor ($NiMoO_4$ plus MoO_3) were, however, significantly different. Under the same reaction conditions (1223 K, 4 h), single-phase Ni_2Mo_3N was identified as the resulting product when the samples are quenched to room temperature. On the other hand, in line with previous observations, slow cooling of samples results in the presence of detectable impurities, which has been attributed to the capability of this system to absorb more nitrogen at low temperatures to give products with a lower total metal to nitrogen ratio.[1,6e] This observation is consistent with the above results concerning the direct ammonolysis of the amorphous precursor. Very likely, more prolonged thermal treatments of the amorphous precursor would lead to the total conversion of the secondary phases in Ni_2Mo_3N. In this sense, however, this procedure is disadvantageous relative to the ammonolysis of the crystalline precursor.

Fig. 1 shows experimental and calculated X-ray diffraction patterns corresponding to pure Ni_2Mo_3N. In contrast to results in ref. 1, EDAX analysis confirms now a homogeneous Ni : Mo = 2 : 3 composition throughout the entire sample, and the nitrogen content (3.34 wt.%, combustion analysis) is also consistent with the Ni_2Mo_3N stoichiometry. No possible impurity attributable to the synthetic procedure (such as C) was detected in any significant amount (*ca.* 0.01 wt.%). Only a very small amount of oxygen was detected (0.19 wt.%).

The morphology of both the crystalline precursor ($NiMoO_4$ plus MoO_3) and Ni_2Mo_3N was observed using scanning electron microscopy. SEM images of the precursor [Fig. 2(a)] show mainly polyhedral faceted particles, with a mean particle size around 250 nm. The final Ni_2Mo_3N powder [Fig. 2(b)] consists of an aggregate of spherical particles with typical diameter around 500 nm. It should be noted that this non-pseudomorphic transformation associated with nitridation is

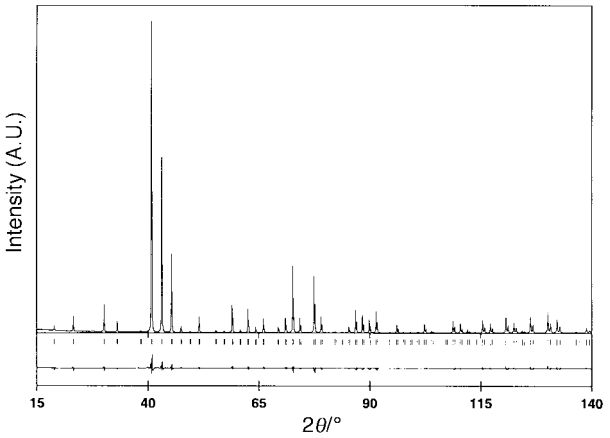

Fig. 1 Observed (dotted) and calculated (solid) X-ray diffraction profile for Ni_2Mo_3N. Tic marks below the diffractogram represent the allowed Bragg reflections. The residual lines are located at the bottom of the figures.

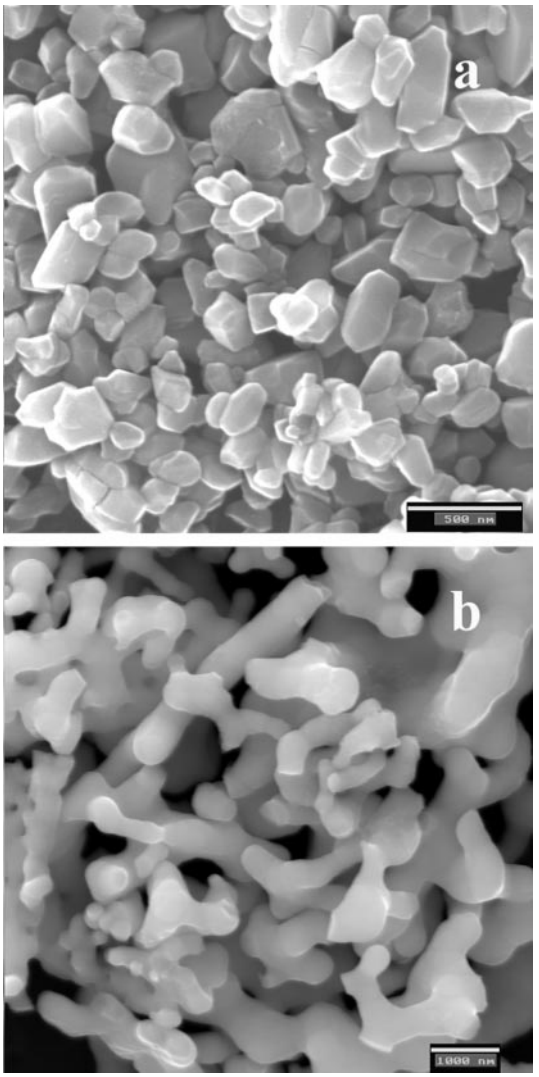

Fig. 2 SEM images showing the microstructure of: (a) crystalline precursor of the Ni_2Mo_3N nitride; (b) Ni_2Mo_3N nitride. Scale bars correspond to 500 and 1000 nm, respectively.

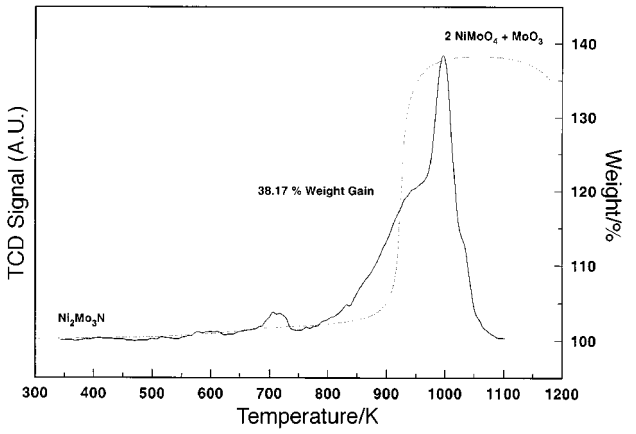

Fig. 3 Characteristic TPO (continuous line) and TGA (broken line) profiles corresponding to Ni_2Mo_3N.

clearly similar to that observed when $NiMoO_4$ was used as precursor,[1] despite the morphological differences between the precursors.

Fig. 3 shows a characteristic TPO profile and TGA curve for Ni_2Mo_3N under air atmosphere up to 1173 K. Although there are quantitative differences between the registered temperatures for the main effects in both experiments (attributable, very likely, to differences in the sample size and ventilation and in the geometric characteristics of the holders),[15] the TGA curve shows that oxidation of the bulk sample (after a continuous slight weight gain) occurs at *ca.* 900–1000 K. The TPO peak associated with this effect in the TGA curve is complex, which suggests that the oxidation process could occur through a multi-step mechanism. The total mass gain associated with this effect, 38.17%, is very close to the theoretical value, 38.64%, corresponding to $Ni_2Mo_3N \rightarrow 2NiMoO_4 + MoO_3$. Also, the final oxidation products were identified as $NiMoO_4$ (JCPDS 33,0948) and MoO_3 (JCPDS 35,0609). This result, which is consistent with the nitrogen analysis, indicates also that the ternary nitride, Ni_2Mo_3N, does not contain appreciable quantities of oxygen. Thus, the synthetic procedure described here guarantees the total nitridation of the precursor ($NiMoO_4$ plus MoO_3) to give Ni_2Mo_3N, which does not suffer significant superficial oxidation by air exposure (contrary to that observed for other ternary nitrides for which passivation is required, see below). Weight losses above 1100 K are due to MoO_3 sublimation.

V–Mo–O–N system

The success of our synthetic strategy for Ni_2Mo_3N led us to consider its applicability for obtaining other related phases of interest. We initially focussed our efforts on $V_2Mo(O_xN_y)$, an oxynitride of cubic structure having remarkable catalytic properties. This oxynitride was first reported by Oyama and coworkers,[9a–e] who described its preparation ($x=1.7$, $y=2.4$; although these nitrogen and oxygen contents could vary with the experimental conditions) by ammonolysis of the bimetallic V_2MoO_8 mixed oxide.[9b] As set out below, by applying our synthetic procedure, we have identified the crystalline precursor (Table 1) of $V_2Mo(O_xN_y)$ as a mixture of $V_9Mo_6O_{40}$ and V_2O_5, which has guided us towards the preparation of $V_3Mo_2(O_xN_y)$, a new vanadium–molybdenum oxynitride also having cubic (NaCl-type) structure.

As described in the experimental section, in order to obtain the V : Mo = 2 : 1 oxynitride, $V_2Mo(O_xN_y)$, we prepared an amorphous freeze-dried precursor having this nominal metal stoichiometry. A deep-green crystalline solid was obtained by heating the amorphous precursor under air (723 K, 3 h). The X-ray diffraction pattern of the resulting product [Fig. 4(a)] allowed identification of both $V_9Mo_6O_{40}$ (JCPDS 34,0527)

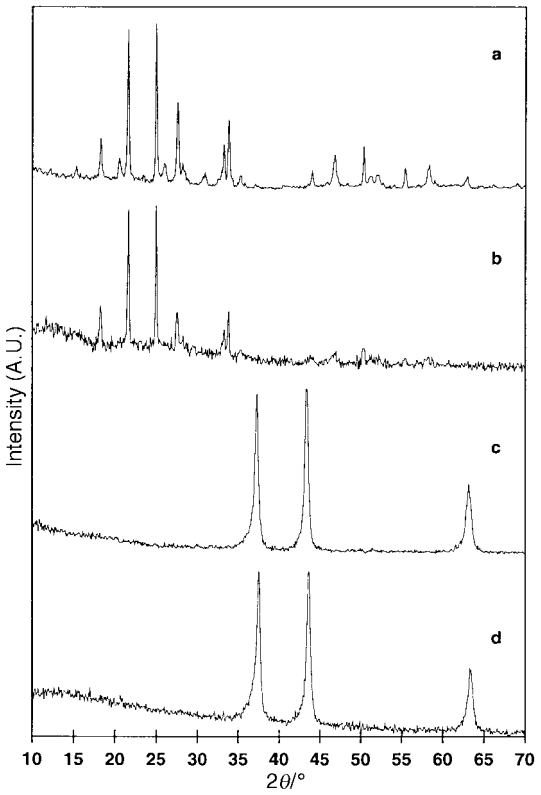

Fig. 4 X-Ray diffraction patterns of: (a) crystalline V : Mo = 2 : 1 precursor; (b) crystalline V : Mo = 3 : 2 precursor; (c) $V_2Mo(O_xN_y)$; (d) $V_3Mo_2(O_xN_y)$.

and V_2O_5 (JCPDS 41,1426). TGA results indicate that decomposition of the amorphous precursor is complete at *ca.* 620 K. As stated above (see synthesis), we also prepared, for comparison, a crystalline V–Mo mixed oxide by the ceramic procedure (starting from an intimate equimolar mixture of V_2O_5 and MoO_3, *i.e.* V : Mo 2 : 1 ratio). The resulting crystalline solid was again identified as consisting of $V_9Mo_6O_{40}$ and V_2O_5. In practice, this result agrees with that predicted from the reported phase diagram for the V_2O_5–MoO_3 system,[16] and is also consistent with the contention of Munch and Pierron[17] that the intermediate ternary mixed oxide in this system is $V_8{}^{V}V^{IV}Mo_6O_{40}$ rather than V_2MoO_8 as reported by Eick and Kihlborg.[18] Actually, the claim of Oyama and coworkers that the crystalline oxide precursor of $V_2Mo(O_xN_y)$ is V_2MoO_8 was based on the XRD analysis of Eick and Kihlborg (JCPDS 20,1377),[18] although the pattern shown in that work[9a] presents clear evidence of preferential orientation. In any case, it should be noted that the conventional solid state reaction described by Oyama and coworkers[9a] was performed at a temperature (948 K) higher than that used in our experiment (873 K). At this point, we prepared an amorphous freeze-dried precursor having a V : Mo = 3 : 2 nominal stoichiometry (Table 1). It was treated as above (723 K, 3 h), and the result was again a deep-green crystalline solid whose XRD pattern [Fig. 4(b)] corresponds to only $V_9Mo_6O_{40}$. These results can not exclude, by themselves, the existence of a hypothetical V_2MoO_8 compound, but they clearly support the assertion that the stable intermediate crystalline mixed oxide in the V_2O_5–MoO_3 system is $V_9Mo_6O_{40}$.[17]

In contrast to Ni_2Mo_3N, the results of ammonolysis processes (1038 K, 2 h) were independent (Table 1) of the amorphous or crystalline character of the V–Mo precursor (for any of the V : Mo stoichiometries). Chemical analyses of samples of the resulting products (black solids) indicate that, in all cases, the V : Mo ratio is (within experimental error) equal to the nominal value in the corresponding precursor, and the

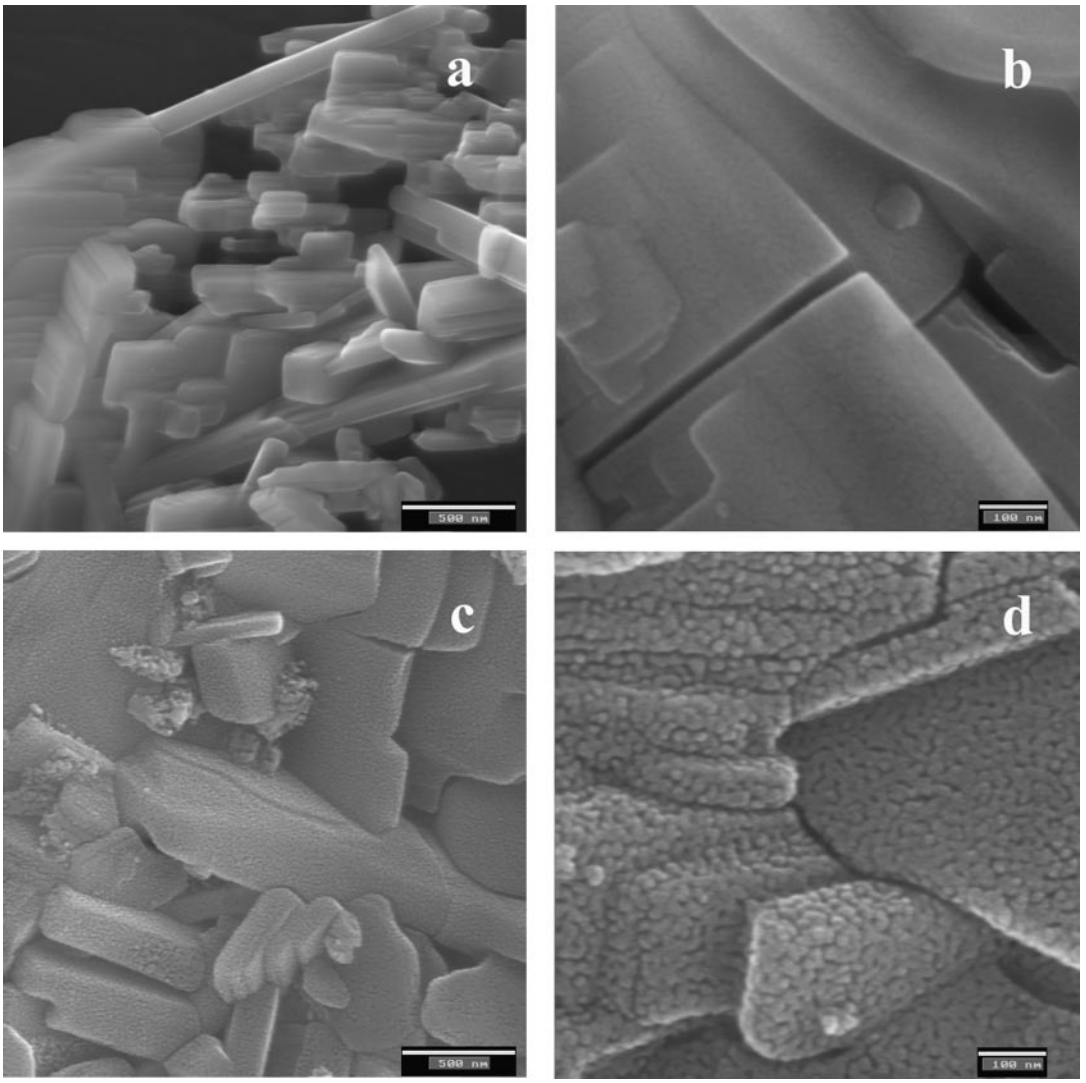

Fig. 5 SEM images showing the microstructure of products with V:Mo = 2:1 metal ratio: (a) and (b), crystalline precursor; (c) and (d), $V_2Mo(O_xN_y)$. Scale bars correspond to 500, 100, 500 and 100 nm, respectively.

final oxynitrides can be formulated as $V_2Mo(O_xN_y)$ and $V_3Mo_2(O_xN_y)$ (see Table 1). In line with previous observations,[9b] nitrogen and oxygen contents can vary to some extent depending on the procedural variables. Both the interstitial character of the non-metal atoms (see below) and possible surface oxidation may be responsible for this constitutional tolerance. Fig. 4 shows characteristic XRD patterns corresponding to both oxynitrides. It must be stressed that both have the same characteristic XRD pattern of the rock salt structure (space group *Fm*3*m*). No other phases were observed. The cell dimensions of the synthesized oxynitrides [4.151(3) and 4.153(3) Å, respectively] are similar to those previously reported for related phases.[9b,e] It is also remarkable that both oxynitrides are isostructural to the individual nitrides VN and Mo_2N,[19] in which the metal atoms occupy a face centered cubic lattice and nitrogen fill octahedral interstitial positions.

Scanning electron microscopy images show that morphological evolution from the precursors to the ternary oxynitrides is very similar for both metal compositions under study. Fig. 5 shows characteristic SEM images corresponding to V:Mo = 2:1. Low temperature (723 K) thermal decomposition of the amorphous freeze-dried precursor leads to [Fig. 5(a)] elongated crystals ($V_9Mo_6O_{40}$ plus V_2O_5), with typical dimensions around $2000 \times 400 \times 200$ nm, which have plane surfaces [as observed at high magnification, Fig. 5(b)]. The external appearance of the crystals remains unchanged during the ammonolysis process (1038 K, 2 h) yielding $V_2Mo(O_xN_y)$ [Fig. 5(c)], although they now show wrinkled surfaces. SEM images at high magnification [Fig. 5(d)] clearly reveal that $V_2Mo(O_xN_y)$ grains are aggregates of nanometric spherical particles with typical diameter around 20 nm. An analogous pseudomorphical evolution was already observed by Oyama and coworkers[9] upon synthesising VN solid foams from V_2O_5.[20] Similar results were obtained when the crystalline mixed oxide precursor ($V_9Mo_6O_{40}$ plus V_2O_5) was prepared by a conventional solid state reaction (Fig. 6). Crystal aggregates (*ca.* 50 μm) with plane surfaces [Fig. 6(a)] maintained their external appearance after nitridation [Fig. 6(b)], but high magnification [Fig. 6(c)] shows again nanometric spherical particles (*ca.* 20 nm).

Fig. 7 shows a characteristic TPO profile and TGA curve for $V_3Mo_2(O_xN_y)$ under air atmosphere up to 900 K. Oxidation of the bulk sample begins now at relatively low temperature (*ca.* 500 K *vs.* 900 K for Ni_2Mo_3N). Both TPO and TGA curves suggest that oxidation occurs in a two step process, the final product of which (863 K) is $V_9Mo_6O_{40}$ (JCPDS 34,0527). $V_2Mo(O_xN_y)$ behaves similarly. Low temperature oxidation is consistent with the pyrophoric character of these products, this making necessary passivation (under N_2 atmosphere) prior to their manipulation. Surface oxidation must account to a great extent for the oxygen content of these oxynitrides.

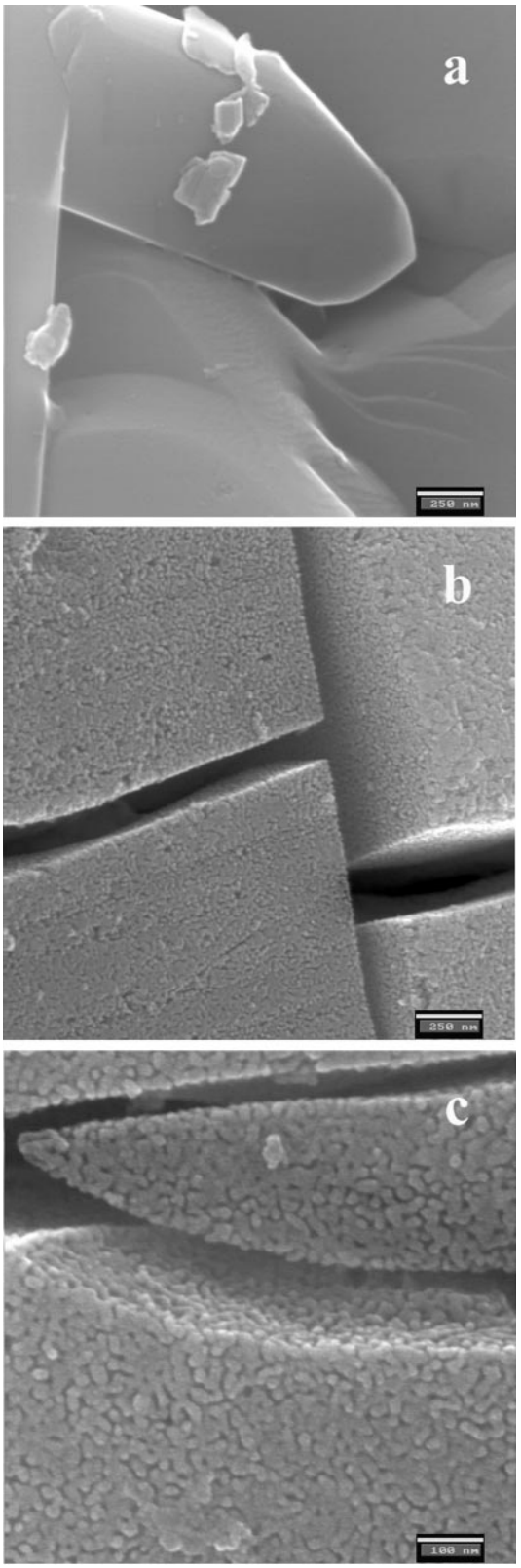

Fig. 6 SEM images showing the microstructure of products with V:Mo = 2:1 metal ratio: (a) ceramic precursor; (b) and (c), $V_2Mo(O_xN_y)$. Scale bars correspond to 250, 250 and 100 nm, respectively.

Concluding remarks

The use of polymetallic precursors resulting from the freeze-drying of aqueous solutions has proved to be a powerful technique to explore different metallic compositions in complex systems such as those dealt with here. Indeed, it has allowed us to overcome stoichiometric problems associated with the use of single mixed oxides as precursors, this making it possible to obtain single-phase Ni_2Mo_3N. In the same way, we have been able to prepare a new metallic composition in the V–Mo–O–N system, $V_3Mo_2(O_xN_y)$. The fact that both this oxynitride and the already known $V_2Mo(O_xN_y)$ present the same NaCl-type structure as that of the VN and Mo_2N individual nitrides, suggests the existence of a solid solution of stoichiometry $V_{1-z}Mo_z(O_xN_y)$ $(0 \leqslant z \leqslant 1)$ having rock salt structure. Thus, $V_2MoO_{1.7}N_{2.4}$ catalyst, which has been referred to as having superb HDN performance with an activity higher than that of VN and Mo_2N,[9a,e,10] should be only one of the possible compositions in the $V_{1-z}Mo_z(O_xN_y)$ solid solution. As far as the catalytic activity in this system must depend on its stoichiometric metal ratio, the synthetic approach reported here opens a way to optimize the HDN catalytic properties in the V–Mo–O–N system. Preliminary results relating to the preparation by this method of different $V_{1-z}Mo_z(O_xN_y)$ $(0 \leqslant z \leqslant 1)$ compositions have been satisfactory, and further study is in progress.[21]

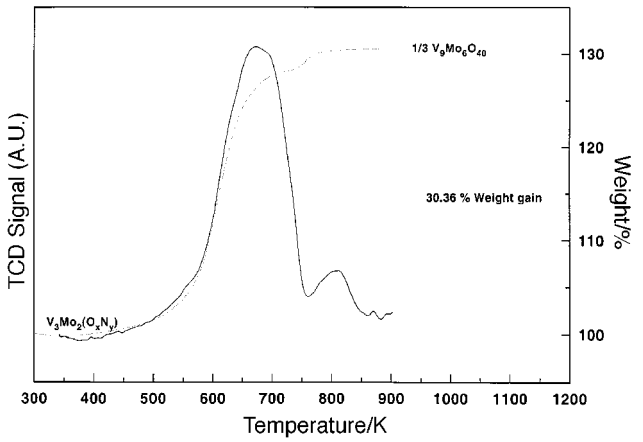

Fig. 7 Characteristic TPO (continuous line) and TGA (broken line) profiles corresponding to $V_3Mo_2(O_xN_y)$.

This research was supported by the Spanish Comisión Interministerial de Ciencia y Tecnología (MAT96–1037). The SCSIE of the Universitat de València is acknowledged for X-ray diffraction and analytical facilities. S. A. acknowledges the Fondo para el Mejoramiento de la Calidad Universitaria (FOMEC) and the Universidad del Litoral for a grant for her stay in Spain.

References

1 S. Alconchel, F. Sapiña, D. Beltrán and A. Beltrán, *J. Mater. Chem.*, 1998, **8**, 1901.
2 *The Chemistry of Transition Metal Carbides and Nitrides*, ed. S. T. Oyama, Blackie Academic & Professional, Chapman & Hall, London, 1996, p. 1; *International Symposium on Nitrides*, in *J. Eur. Ceram. Soc.*, ed. Y. Laurent and P. Verdier, 1997, vol. 17, pp. 1773–2037.
3 *High surface area nitrides and carbides*, in *Catal. Today*, ed. P. W. Lednor, 1992, vol. 15.
4 V. Cortés-Corberán, *Prog. Catal.*, 1997, **6**, 113.
5 H. C. zur Loye, J. D. Houmes and D. S. Bem, in *The Chemistry of Transition Metal Carbides and Nitrides*, ed. S. T. Oyama, Blackie Academic & Professional, Chapman & Hall, London, 1996, p. 154.
6 (*a*) S. H. Elder, L. H. Doerrer, F. J. DiSalvo, J. B. Parise, D. Gouyomard and J. M. Tarascon, *Chem. Mater.*, 1992, **4**, 928; (*b*) D. S. Bem and H. C. zur Loye, *J. Solid State Chem.*, 1993, **104**, 467; (*c*) J. D. Houmes, D. S. Bem and H.-C. zur Loye, *MRS Symposium Proceedings: Covalent Ceramics II: Non-Oxides*, ed. A. R. Barron, G. S. Fischman, M. A. Fury and A. F. Hepp, Materials Research Society, Boston, MA, 1993, vol. 327, p. 153; (*d*) D. S. Bem, C. P. Gibson and H.-C. zur Loye, *Chem. Mater.*, 1993, **5**, 397; (*e*) D. S. Bem, H. P. Olsen and H.-C. zur Loye, *Chem.*

Mater., 1995, **7**, 1824; (*f*) P. Subramanya Herle, N. Y. Vasanthacharya, M. S. Hedge and J. Gopalakrishnan, *J. Alloys Compd.*, 1995, **217**, 22; (*g*) D. S. Bem, C. M. Lampe-Onnerud, H. P. Olsen and H.-C. zur Loye, *Inorg. Chem.*, 1996, **35**, 581; (*h*) R. N. Panda and N. S. Gajbhiye, *J. Alloys Compd.*, 1997, **256**, 102.

7 K. S. Weil and P. N. Kumta, (*a*) *Mater. Sci. Eng. B*, 1996, **38**, 109; (*b*) *J. Solid State Chem.*, 1997, **128**, 185; (*c*) 1997, **134**, 302; (*d*) *Acta Crystallogr., Sect. C*, 1997, **53**, 1745; (*e*) P. Subramanya Herle, M. S. Hedge, K. Sooryanarayana, T. N. Guru Row and G. N. Subbanna, *J. Mater. Chem.*, 1998, **8**, 1435.

8 V. Primo, F. Sapiña, M. J. Sanchis, R. Ibañez, A. Beltrán and D. Beltrán, *Solid State Ionics*, 1993, **63–65**, 872.

9 (*a*) C. C. Yu, S. Ramanathan, F. Sherif and S. T. Oyama, *J. Phys. Chem.*, 1994, **98** 13038; (*b*) C. C. Yu and S. T. Oyama, *J. Solid State Chem.*, 1995, **116**, 205; (*c*) C. C. Yu and S. T. Oyama, *J. Mater. Sci.*, 1995, **30**, 4037; (*d*) R. Kapoor, S. T. Oyama, B. Frühberger and J. G. Chen, *J. Phys. Chem. B*, 1997, **101**, 1543; (*e*) C. C. Yu, S. Ramanathan and S. T. Oyama, *J. Catal.*, 1998, **173**, 1; (*f*) S. Ramanathan, C. C. Yu and S. T. Oyama, *J. Catal.*, 1998, **173**, 10.

10 S. T. Oyama, C. C. Yu and F. G. Sherif, *US Pat.* 5 444 173, 1995.

11 J. Rodriguez-Carvajal, FULLPROF Program, personal communication.

12 J. F. Berar and P. Lelann, *J. Appl. Crystallogr.*, 1991, **24**, 1; J. F. Berar, *Acc. in Powder Diffraction II*, *NIST Special Publ.*, 1992, **846**, 63.

13 V. Primo, DRXWin & CreaFit version 2.0: graphical and analytical tools for powder XRD patterns, *ICDD Powder Diffract. J.*, in press.

14 While preparing the present manuscript, Herle *et al.* have reported the isolation of Ni_2Mo_3N by ammonolysis of a metallorganic hydroxide precursor; P. Subramanya Herle, M. S. Hedge, K. Sooryanarayana, T. N. Guru Row and G. N. Subbanna, *Inorg. Chem.*, 1998, **37**, 4128.

15 P. Amorós, R. Ibañez, A. Beltrán, D. Beltrán, A. Fuertes, P. Gomez-Romero, E. Hernandez and J. Rodriguez-Carvajal, *Chem. Mater.*, 1991, **3**, 407.

16 A. Bielanski, K. Dyrek, J. Pozniczek and E. Wenda, *Bull. Acad. Pol. Sci., Ser. Sci. Chim.*, 1971, **19**, 507.

17 R. H. Munch and E. D. Pierron, *J. Catal.*, 1964, **3**, 406.

18 H. A. Eick and L. Kihlborg, *Acta Chem. Scand.*, 1966, **20**, 1658.

19 A. F. Wells, *Structural Inorganic Chemistry*, Clarendon Press, Oxford, 1975, p. 1053.

20 S. T. Oyama, R. Kapoor, H. T. Oyama, D. J. Hofmann and E. Matijevic, *J. Mater. Res.*, 1993, **8**, 1450.

21 A. El-Himri, M. Cairols, S. Alconchel, F. Sapiña, R. Ibañez, A. Beltrán and D. Beltrán, in preparation.

Paper 8/08697D